ISSN 1674-1056
http://cpb.iphy.ac.cn
http://iopscience.iop.org/cpb
中国物理 B
Chinese Physics
中国物理 Chinese Physics B

Electro-optical dual modulation on resistive switching behavior in $BaTiO_3/BiFeO_3/TiO_2$ heterojunction

Jia-Jia Zhao(赵佳佳)[1], Jin-Shuai Zhang(张金帅)[2], Feng Zhang(张锋)[3], Wei Wang(王威)[1], Hai-Rong He(何海蓉)[1], Wang-Yang Cai(蔡汪洋)[1], Jin Wang(王进)[1]

Citation: Chin. Phys. B . 2019, 28(12): 126801 . **doi:** 10.1088/1674-1056/ab54b4
Journal homepage: http://cpb.iphy.ac.cn; http://iopscience.iop.org/cpb

What follows is a list of articles you may be interested in

Emerging properties of two-dimensional twisted bilayer materials

Yang Cheng(程阳), Chen Huang(黄琛), Hao Hong(洪浩), Zixun Zhao(赵子荀), Kaihui Liu(刘开辉)

Chin. Phys. B . 2019, 28(10): 107304 . **doi:** 10.1088/1674-1056/ab3e46

Energy band alignment at Cu_2O/ZnO heterojunctions characterized by *in situ* x-ray photoelectron spectroscopy

Yan Zhao(赵妍), Hong-Bu Yin(尹泓卜), Ya-Jun Fu(符亚军), Xue-Min Wang(王雪敏), Wei-Dong Wu(吴卫东)

Chin. Phys. B . 2019, 28(8): 087301 . **doi:** 10.1088/1674-1056/28/8/087301

Analysis of displacement damage effects on bipolar transistors irradiated by spallation neutrons

Yan Liu(刘岩), Wei Chen(陈伟), Chaohui He(贺朝会), Chunlei Su(苏春垒), Chenhui Wang(王晨辉), Xiaoming Jin(金晓明), Junlin Li(李俊霖), Yuanyuan Xue(薛院院)

Chin. Phys. B . 2019, 28(6): 067302 . **doi:** 10.1088/1674-1056/28/6/067302

Evolutionary algorithm for optimization of multilayer coatings

Mahdi Ebrahimi, Mohsen Ghasemi, Zeinab Sajjadi

Chin. Phys. B . 2018, 27(10): 106802 . **doi:** 10.1088/1674-1056/27/10/106802

Optoelectronic properties of bottom gate-defined in-plane monolayer WSe_2 p-n junction

Di Liu(刘頓), Xiao-Zhuo Qi(祁晓卓), Kuei-Lin Chiu(邱奎霖), Takashi Taniguchi, Xi-Feng Ren(任希锋), Guo-Ping Guo(郭国平)

Chin. Phys. B . 2018, 27(8): 087303 . **doi:** 10.1088/1674-1056/27/8/087303

Electro-optical dual modulation on resistive switching behavior in $BaTiO_3/BiFeO_3/TiO_2$ heterojunction*

Jia-Jia Zhao(赵佳佳)[1], Jin-Shuai Zhang(张金帅)[2], Feng Zhang(张锋)[3], Wei Wang(王威)[1,†], Hai-Rong He(何海蓉)[1], Wang-Yang Cai(蔡汪洋)[1], and Jin Wang(王进)[1]

[1] *School of Computer and Communication Engineering, Changsha University of Science and Technology, Changsha* 410114, *China*
[2] *School of Engineering and Materials Science, Queen Mary University of London, London E*1 4*NS, United Kingdom*
[3] *Peking University Shenzhen Graduate School, Shenzhen* 518055, *China*

(Received 8 August 2019; revised manuscript received 4 October 2019; published online 22 November 2019)

The novel $BaTiO_3/BiFeO_3/TiO_2$ multilayer heterojunction is prepared on a fluorine-doped tinoxide (FTO) substrate by the sol–gel method. The results indicate that the Pt/$BaTiO_3/BiFeO_3/TiO_2$/FTO heterojunction exhibits stable bipolar resistive switching characteristic, good retention performance, and reversal characteristic. Under different pulse voltages and light fields, four stable resistance states can also be realized. The analysis shows that the main conduction mechanism of the resistive switching characteristic of the heterojunction is space charge limited current (SCLC) effect. After the comprehensive analysis of the band diagram and the *P–E* ferroelectric property of the multilayer heterojunction, we can deduce that the SCLC is formed by the effect of the oxygen vacancy which is controlled by ferroelectric polarization-modulated change of interfacial barrier. And the effective photo-generated carrier also plays a regulatory role in resistance state (RS), which is formed by the double ferroelectric layer $BaTiO_3/BiFeO_3$ under different light fields. This research is of potential application values for developing the multi-state non-volatile resistance random access memory (RRAM) devices based on ferroelectric materials.

Keywords: ferroelectric multilayer heterojunction, resistive switching characteristic, electro-optical dual modulation, multi-state resistance

PACS: 68.65.Ac, 73.40.Lq, 85.50.Gk **DOI:** 10.1088/1674-1056/ab54b4

1. Introduction

Recently, with further research on the next generation of non-volatile memory, resistance random access memory (RRAM) is widely considered as a strong competitor to replace the current main stream charge-based floating gate flash memory due to its simple structure, low power consumption, high storage density, fast programming/erase speed, compatible to the complementary metal–oxide semiconductor (CMOS) process, and many other advantages.[1,2] It is no doubt that there is much room for developing it as a kind of memory with non-charge storage mechanism in the following 32-nm technology nodes. At present, materials with resistive switching characteristics have been found to be mainly concentrated in metal oxide, such as HfO_2, NiO, TiO_2, and so on.[2–5] Among all functional thin film materials, ferroelectric compounds with perovskite structure have also attracted great attention in RRAM, such as $BiFeO_3$ (BFO),[6–8] $BaTiO_3$ (BTO),[9,10] and $Bi_{4-x}Nd_xTi_3O_{12}$ (BNT),[11] and so on. Because these compounds have ferroelectric, dielectric, and photovoltaic effects at the same time, which can enrich the research contents of RS and expand its application fields and methods, then they gradually become a hot topic of RRAM.[12,13] In particular, the BFO is the most concerned in them because of its superior ferroelectric and multiferroelectric behaviors.[13,14]

Study on ferroelectric RS behavior was most carried out on the basis of electrode/ferroelectric thin film/electrode sandwich structure,[15–17] while other studies have shown that the structure can significantly improve the RS behavior by introducing suitable insertion layer and providing oxygen vacancy in the RS layer, and can also improve the stability of conductive filament formation and fracture.[18–20] Ma *et al.* studied[16] the multilayer structure of $TiO_2/BaTiO_3/TiO_2$, indicating that the TiO_2 layer formed a large number of oxygen vacancies and the introduction of $TiO_2/BaTiO_3$ interface layers plays a crucial role in determining the bipolar RS behaviors with high consistency and stability.[21] However, in the current research work, there are few RRAM studies based on the combination of metal oxide and ferroelectric materials or the excellent unique characteristics of using multilayer ferroelectric thin films.

At the same time, the research on RS characteristics is mainly for the single regulation mechanism of electro-resistance modulation, and the realization of the optical-resistance modulation characteristics has gradually attracted one's attention.[12,13] For Au/BFO/LSMO/STO heterojunc-

*Project supported by the Scientific Research Program of Hunan Provincial Education Department, China (Grant No. 18C0232) and the International Cooperative Extension Program of Changsha University of Science and Technology, China (Grant No. 2019IC35).

†Corresponding author. E-mail: wangwei@csust.edu.cn

© 2019 Chinese Physical Society and IOP Publishing Ltd

tion, Zhang *et al.* obtained the high and low resistance state through the modulation of pulse voltage with reverse polarization, and the R_H/R_L ratio can be modulated by controlling the illumination condition, which indicates that the electro-resistance dual modulation on RS characteristic is closely related to photovoltaic response.[22] It has been reported in the literature[21] that the BFO/BTO multilayer structure can obviously enhance the ferroelectric and photovoltaic response properties. Therefore, ultimately, it is quite probable to achieve electro-optical dual modulation of the resistive switching behavior by taking advantage of the ferroelectric polarization properties and light response characteristics of ferroelectric materials.

In this work, the BTO/BFO dual film is used as a ferroelectric RS material to improve ferroelectric properties and light absorption efficiency and compared with the mono-layer ferroelectric film,[21,22] thus improving the efficiency characteristics of electro-optical dual modulation on RS behavior. And a TiO_2 film acts as an oxygen vacancy layer which can stabilize the heterostructure RS behavior. The heterojunction of BTO/BFO/TiO_2 (BFT) is prepared by sol–gel technique of low preparing cost, then the electro-optical dual modulation on RS behavior of the heterostructure is further studied.

2. Experimental procedures

The BFO, BTO, and TiO_2 multilayers were prepared by the sol–gel method, and the preparation process details of BFO and BTO precursors were described in the relevant literature.[23,24] The prepared TiO_2, BFO, and BTO precursors were sequentially coated on the FTO substrate by spin coating technology. The details of preparing the multilayer heterojunction of BTO/BFO/TiO_2 and annealing process can be found in Ref. [21]. The independent BFO and BTO films for comparative study were prepared respectively by using the same preparation process.

A square Pt top electrode of 0.5 mm ×0.5 mm was patterned on the as-prepared sample film surface with a shadow mask, by using direct current (DC) magnetron sputtering at an ambient temperature. The crystallographic structure and film cross-section were confirmed by x-ray diffraction (XRD, D8 Advance, Bruker AXS, German) and scanning electron microscope (SEM), respectively. The sample RS characteristics were measured under light condition by using Keithley 4200-SCS. The polarization–voltage (P–V) hysteresis loops of ferroelectric films were obtained by a precise ferroelectric analyzer.

3. Results and discussion

Figure 1(a) shows the XRD patterns of functional layers and the multilayer heterojunction prepared on FTO substrates. The good polycrystals of these films are shown according to the characteristic peaks of the XRD spectrum with a pure phase. The BFO film has a typical hexagonal $R3c$ space group. The TiO_2 and BTO films have a typical anatase structure and a perovskite tetragonal structure, respectively. The characteristic peaks of the BFO, TiO_2, and BTO films all appear in the XRD patterns of the multilayer heterojunction, indicating that all layers of the films coexist in the heterojunction. Meanwhile, according to the results in Ref. [21], the BFO and BTO films show thickness of about 280 nm and 200 nm, respectively, and clear grain profiles can be determined from the cross-sectional image, which indicates that these films have good crystallization.

Figure 1(b) shows the typical ferroelectric P–E hysteresis loop of the BFO film, BTO film, and the BFT heterojunction under the same conditions, where the inset shows the diagram of the structure and the electrical test of the device. The figure shows that the remanent polarization (P_r) of the BFO/BTO/TiO_2 heterostructure is of 11 μC/cm^2, much higher than those of the single BFO and/or BTO film, and the coercive field voltage (V_c) is 3.1 V. The improvement of the BFT heterojunction ferroelectric properties may be related to the small leakage current characteristics of BTO film, which acts as an insulating barrier between BFO film and Pt electrode,[24,25] which can limit the leakage current of the BFO film, resulting in a large polarization and superior ferroelectric properties. However, the enhancement of the ferroelectric properties of the heterojunction may also be related to interface stress caused by the multilayers.[21,24,26]

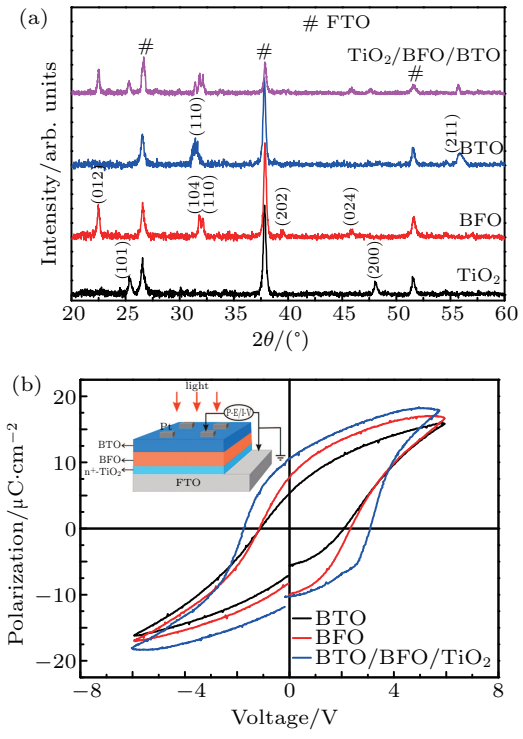


Fig. 1. (a) XRD patterns and (b) room temperature ferroelectric P–E hysteresis curves of bare BFO and BTO thin films and multilayered BFT structure.

The RS properties of the BFT heterojunction are illustrated in Fig. 2. Figure 2(a) shows a typical RS characteristic loop of the device, and the applied voltage sweep follows the sequence: -4 V$\rightarrow$ 0 V$\rightarrow$ $+4$ V$\rightarrow$ 0 V$\rightarrow$ -4 V forward (reverse) bias is defined as a positive voltage applied to the bottom (top) FTO electrode, corresponding to polarization direction forward (downward), where the direction of arrow is marked in turn, we can see that the structure shows bipolar RS behavior from the *I*–*V* semi-logarithmic scale loop. With the increase of forward bias, the sudden increase of current occurs at about $+3.2$ V, and the switch resistance state changes from high-resistance state (HRS) to low-resistance state (LRS) (defined as the SET process), so we can infer that its changes are associated with ferroelectric polarization characteristics of the structure. And when the applied voltage sweep follows the sequence of 0 V$\rightarrow -4$ V$\rightarrow$ 0 V, the RS characteristic turns from LRS to HRS (defined as the RESET process). It is worth mentioning that the existence of defects concentrates some charges in positive electric field, and these charges will form pinning effect on polarization in electric field reverse, resulting in the reversible polarization decreasing and the *I*–*V* loop opening at -4 V. At the same time, the asymmetry between the upper and the lower interface in the sample can also make the SET voltage and Reset voltage asymmetric, so the reset voltage of the heterojunction will be lower than -4 V.

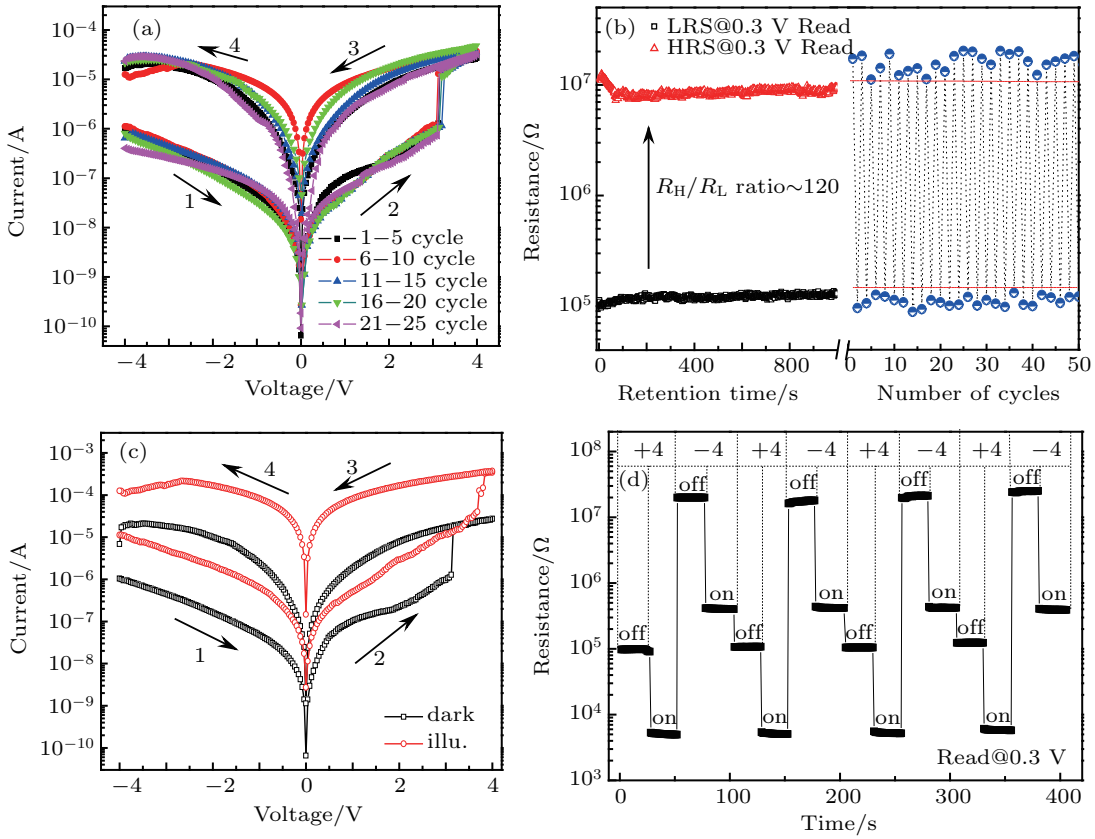


Fig. 2. (a) The *I*–*V* curves on semi-log scales for as-prepared Pt/BFT/FTO samples with 25 consecutive cycles, (b) device retention and fatigue characteristics at ON/ OFF states, (c) RS characteristic under dark field and light conditions for as-prepared samples by increasing voltage sweep range, with black symbols being for the *I*–*V* curves in dark, and the red symbols the *I*–*V* curves under illumination, and (d) variations in the junction resistances of the heterojunction with $\pm$4 V pulse voltage measured at 0.3 V in dark and illumination (illu.) conditions.

The SET-RESET process is repeated for more than 25 cycles under dark condition, and the results show that the BFT device has high uniformity and stability of RS behavior. The retention characteristics of HRS and LRS of the device are shown in Fig. 2(b), where the voltage of all the resistance values is $+0.3$ V (see red curve). The resistance ratio of R_H/H_L is about 120 with good retention, and the result is better than the ratio of $TiO_2/BaTiO_3/TiO_2$ (about 10) reported by Ma *et al.*[16] Neither the resistance value of HRS nor the resistance value of LRS is obviously degenerative in the retention time of 10^3 s, indicating the non-volatile characteristics. With the retention time increasing, the currents of the LRS and HRS show their fluctuation behavior. This current fluctuation may be due to the migration of oxygen vacancies as explained in the literature.[21] As shown in the right part of Fig. 2(b), the device's HRS and LRS have almost no degradation after 50 flips, indicating that the excellent non-volatile and anti-fatigue characteristics of the device, which can meet the requirements for information storage. The *I*–*V* loops of the Pt/BFT/FTO heterojunction under the dark and illumination condition are shown in Fig. 2(c). The current loops under the illumination (red curve, the light source wavelength

is in a range of 330 nm–780 nm centered at 512 nm with the power of 30 mW/cm^2) obviously increase, indicating the photo-resistance effect. To further study the electro-optical dual modulation on the RS behavior, the junction resistance time dependence property of the Pt/BFT/FTO heterojunction in ±4 V pulse polarization voltage and in dark condition and illumination condition are measured with the read voltage of +0.3 V as shown in Fig. 2(d). Therefore, four stable resistance states can be achieved.

Compared with the models of several RS mechanisms currently accepted, several conductive models are used to fit the typical I–V data of HRS and LRS to understand the possible conduction mechanism of RS behavior. As shown in Fig. 3(a), the ln(I)–ln(V) curve of HRS on the semi-log scale shows that the linear fitting result of the current behavior exhibits Ohmic conduction mechanism in low voltage region (0 V–0.3 V), and the linear slope of its current with respect to voltage is 1.1. The slope of voltage region (0.2 V–2 V) is 1.7, which is approximately $I \propto V^2$ ($n \approx 2$)[7] and can be regarded as satisfying the Child Law. In high voltage region (2 V–3.2 V), the slope is increased to 4.6, and based on this, SCLC conduction mechanism can be explained.[5,27] As for the LRS under positive bias, Schottky emission dominates the current, which is confirmed by ln(I) ∝ Sqrt(V)[28] (Fig. 3(b)), indicating that Schottky barrier exists at the interface of multilayer heterojunction.

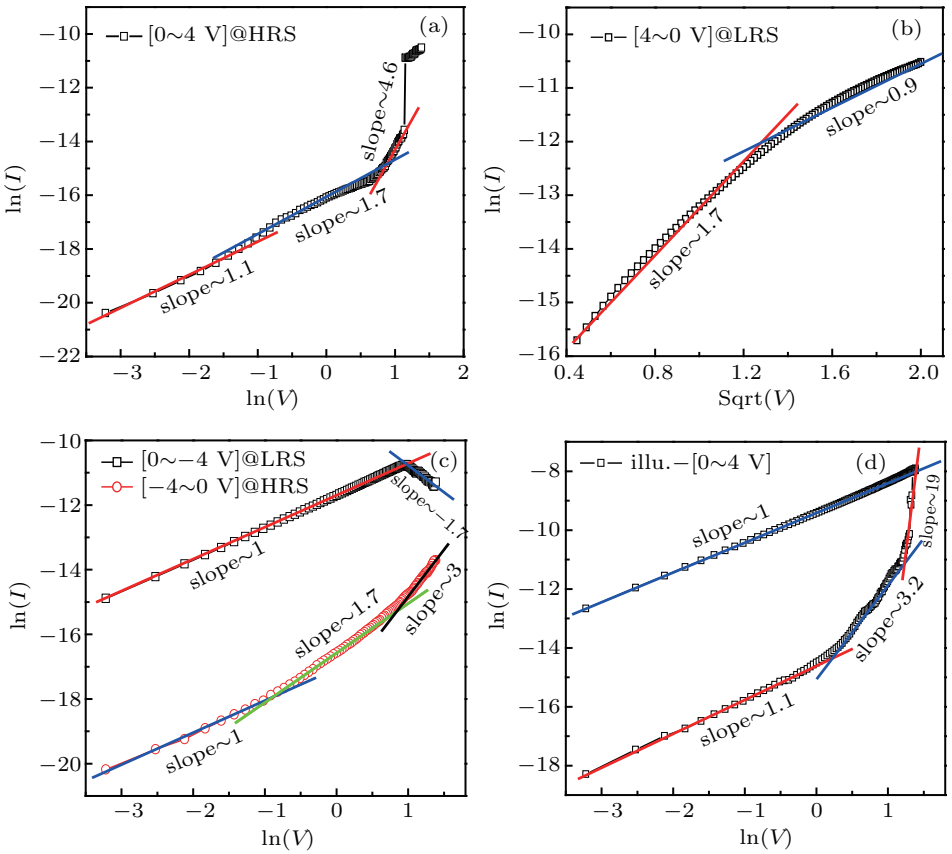


Fig. 3. I–V curves in Figs. 2(a) and 2(c) to reveal their conduction mechanisms: (a) ln(I) *versus* ln(V) at HRS and (b) ln(I) *versus* Sqrt(V) at LRS in positive bias range (0 V–4 V), (c) ln(I) *versus* ln(V) in negative bias range (−4 V–0 V), and (d) ln(I) *versus* ln(V) in positive bias region under illumination.

As shown in Fig. 3(c), the ln(I)–ln(V) relationship in the negative bias range: its HRS exhibits Ohmic conduction mechanism in the low voltage range, while the LRS exhibits a Child conductance range and a linear relationship of $I \propto V^3$ in the high voltage range. This indicates that the negative bias range also affects the SCLC conduction mechanism. The LRS is mainly an Ohmic conduction mechanism, and a negative differential resistance occurs in the high voltage range, which also satisfies the SCLC conduction mechanism. This is consistent with previously reported interface RS effect that oxygen vacancy migration and carrier injection near the interface play an important role in RS.[29] Figure 3(d) shows the LRS ln(I)–ln(V) linear relationship with a slope of 1 in the positive bias region under illumination, indicating that the LRS is completely consistent with the Ohmic conductance mechanism. The ln(I)–ln(V) of HRS exhibits a piecewise linear relationship: the slope is 1 in the low voltage region, which is also Ohmic behavior. When the voltage becomes slightly higher, the slope increases, indicating that the conductivity mechanism of HRS is the SCLC conduction mechanism. In view of the above, the RS characteristics of the Pt/BFT/FTO heterojunction device are the result of the combination of the bulk-limited conductance mechanism controlled by Ohmic conductance and SCLC conduction and the interface-limited mecha-

nism controlled by Schottky emission effect.

Based on the above detailed experimental results, the ferroelectric polarization modulation effect on the depletion layer width and the film interface barrier height are considered to explain the RS behaviors observed in the Pt/BFT/FTO heterojunction. Since the work function of BTO (5.26 eV)[30] and TiO_2 (4.1 eV)[31] are close to that of Pt and FTO[12] respectively, it can be considered that both the Pt/BTO and TiO_2/FTO interface form a similar flat-band Ohmic contact. Due to the volatilization of Bi ions, a p–n junction is formed at the BFO/TiO_2 interface between n-type TiO_2[31] and p-type BFO,[32] and its built-in field ($\boldsymbol{E}_{b1}$) direction is from TiO_2 to BFO. Since the work function of BTO is greater than that of BFO (WBFO = 4.7 eV),[14,33] the interface of BFO/BTO will form a barrier. Therefore, the BFT heterojunction forms two interface electric fields $\boldsymbol{E}_{b1}$ and $\boldsymbol{E}_{b2}$ in the same direction, and the direction is from FTO to Pt as shown in Fig. 4(a).

The randomness of ferroelectric polarization does not contribute to ferroelectric polarization in the initial state, but an interface barrier can be formed due to the difference in carrier concentration and the difference in work function at the interface. And n-type TiO_2 is easy to form a large number of oxygen vacancies after being annealed, while the oxygen vacancies are of crucial importance in reversible process of RS behavior.[16,18,30]

When the ferroelectric polarization is upward by applying a forward voltage (the bottom electrode FTO applied +6 V bias), the negative polarization bound charges will accumulate at the interface of TiO_2/BFO, and the positively charged oxygen vacancies in TiO_2 drift to the interface of TiO_2/BFO, while the electrons provided by the top electrode Pt pass through the BTO and BFO layers into the interface of TiO_2/BFO, and are bound by the oxygen vacancies at the interface as shown in the Fig. 4(a) which corresponds to the *I*–*V* characteristics of the SCLC mechanism in the forward region in Fig. 3(a). The depletion layer width of TiO_2/BFO and BFO/BTO interface are narrowed under the positive polarization, and the lower barrier makes the carrier transition easier to change (as shown in Fig. 4(c)). When a sufficiently high forward bias is applied to a heterojunction, the oxygen vacancies under the action of the electric field, can cross the interface and enter into the ferroelectric layer, and migrate toward and accumulate at the top electrode of Pt, where TiO_2 is the source of a large number of oxygen vacancies as shown in Figs. 3(c) and 3(d). Finally, the conductive path from the bottom electrode FTO to the top electrode Pt is realized and the LRS is gradually formed, which is the reason why the current presents a sharp increase at 3.2 V as shown in Fig. 2(a). Due to the function of BTO and BFO ferroelectric films, the bound electrons cannot be released randomly, so the samples show non-volatile property.

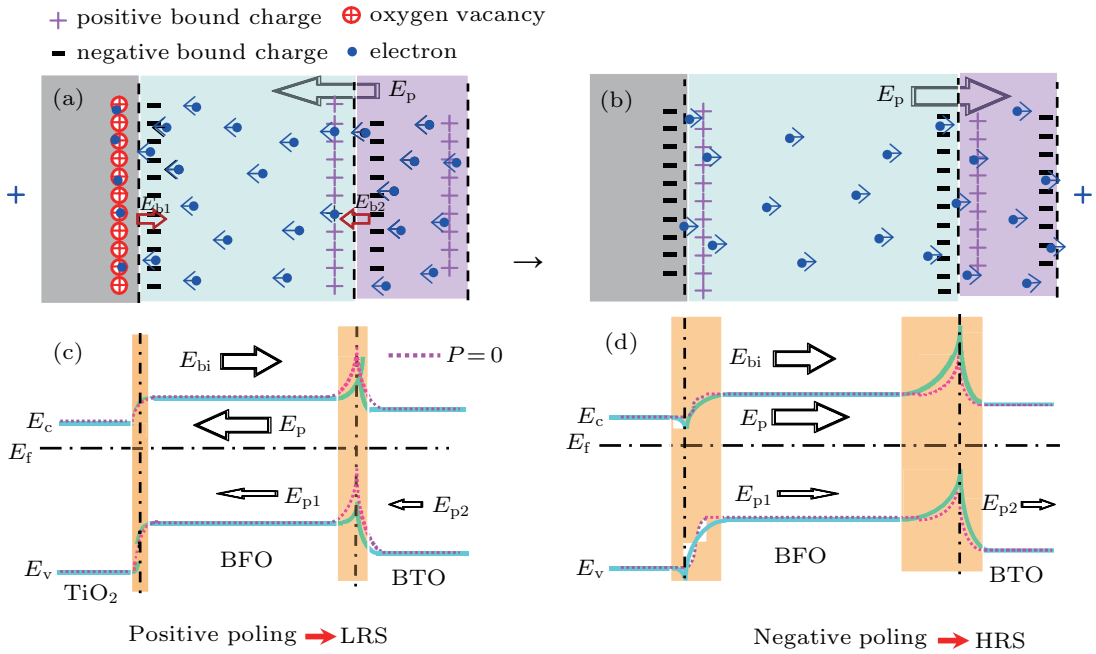


Fig. 4. (a) and (c) Formation of LRS and energy-band of Pt/BFT/FTO heterojunction at LRS under dark condition. (b) and (d) Formation of HRS and energy-band of Pt/BFT/FTO heterojunction at HRS under dark condition.

When the ferroelectric polarization is downward by applying a reverse voltage (+6 V bias is applied to the top electrode Pt), the bound electrons in oxygen vacancies are released, and the ferroelectric positive bound charges are transferred to the TiO_2/BFO interface. The oxygen vacancies at the TiO_2/BFO interface drift back to the TiO_2 region, and the conductive filament ruptures at the interface of TiO_2/BFO,[21] as shown in Fig. 4(b). At the same time, the built-in field increases and the depletion region at the interface of TiO_2/BFO and BFO/BTO widen, accompanied with up-

ward band bending and enhanced Schottky barrier, that is, the carriers are not easy to migrate, switching the cell back to the HRS (Fig. 4(d)).Therefore, the oxygen vacancies migrating at TiO_2/$BaTiO_3$ interface can be stabilized to form and rupture the filament, thereby forming highly uniform RS characteristics. In a word, it explains that the heterojunction achieves the modulation of RS behavior by ferroelectric polarization.

When the BTO/BFO/TiO_2 heterojunction absorbs the light energy greater than the band-gaps of the material, it forms effective photo-induced electron–hole pairs, which are separated by the build-in field and the depolarization field. As shown in Fig. 2(c), another two resistance states can be formed respectively under dark and illumination condition.[12,24] Therefore, based on different polarization states and light conditions, four different stable resistance states can be realized as shown in Fig. 2(d).

4. Conclusions

In summary, we construct a Pt/BTO/BFO/TiO_2/FTO heterojunction by using the sol–gel method. The resistive properties of the structure are studied, and the bipolar stable resistance with good retention characteristics is also obtained. The pulse voltage with alternately opposite polarization directions is used to realize the inversion of the resistive state of the device, and the high- and low-resistances can be changed by the light switch, thereby realizing the stable multi-stage resistance state and the combination of the light-resistance and the electric-resistance modulation effect. The resistive mechanism of the structure can be summarized as follows: the SCLC effect is controlled by oxygen vacancy defects, the depletion layer and barrier height of the interface are regulated by different polarization electric fields, and thus producing a new additional resistance of photo-controlled photo-generated carriers. The state increases the new dimension of device resistance state regulation. Therefore, this study paves a new way for the potential application of non-volatile resistance memory with ferroelectric multi-configuration modulation.

References

[1] Odagawa A, Katoh Y, Kanzawa Y, Wei Z and Mikawa T 2007 *Appl. Phys. Lett.* **91** 133503

[2] Kim D C, Seo S, Ahn S E, Suh D S, Lee M J, Park B H, Yoo I K, *et al.* 2006 *Appl. Phys. Lett.* **88** 202102

[3] Kwon D H, Kim K M, JangJ H, Jeon J M, Lee M H, Kim G H and Kim M 2010 *Nat. Nanotechnol.* **5** 148

[4] Zhao M, Zhu Y, Wang Q, Wei M, Liu X, Zhang F and Xiong R 2016 *Appl. Phys. Lett.* **109** 013504

[5] Meng Y, Zhang P J, Liu Z Y, *et al.* 2010 *Chin. Phys. B* **19** 037304

[6] Yan T L, Chen B, Liu G, *et al.* 2017 *Chin. Phys. B* **26** 067702

[7] Luo J M, Lin S P, Zheng Y and Wang B 2012 *Appl. Phys. Lett.* **101** 062902

[8] Gong Y F, Wu P, Liu W F, *et al.* 2012 *Chin. Phys. Lett.* **29** 047701

[9] Jung C H, Woo S I, Kim Y S and No K S 2011 *Thin Solid Films* **519** 3291

[10] Yan Z, Guo Y, Zhang G and Liu J M 2011 *Adv. Mater.* **23** 1351

[11] Song H J, Wang J B, Zhong X L, Cheng J J, Jia L H, Wang F and Li B 2013 *Appl. Phys. Lett.* **103** 262901

[12] Wang L, Jin K J, Ge C, Wang C, Guo H Z, Lu H B and Yang G Z 2013 *Appl. Phys. Lett.* **102** 252907

[13] Qu T L, Zhao Y G, Xie D, Shi J P, Chen Q P and Ren T L 2011 *Appl. Phys. Lett.* **98** 173507

[14] Yang H, Luo H M, Wang H, Usov I O, Suvorova N A, Jain M, Feldmann D M, Dowden P C, Depaula R F and Jia X 2008 *Appl. Phys. Lett.* **92** 102113

[15] Waser R, Dittmann R, Staikov G and Szot K 2009 *Adv. Mater.* **21** 2632

[16] Ma W J, Lin S P, Luo J M, Zhang X Y, Wang Y, Li Z X, Wang B and Zheng Y 2013 *Appl. Phys. Lett.* **103** 262903

[17] Hasegawa T, Terabe K, Tsuruoka T and Aono M 2012 *Adv. Mater.* **24** 252

[18] Do Y H, Kwak J S, Bae Y C, Jung K, Im H and Hong J P 2009 *Appl. Phys. Lett.* **95** 093507

[19] Lee M J, Lee C B, Lee D, Lee S R, Chang M, Ji H H, Young B K, *et al.* 2011 *Nat. Mater.* **10** 625

[20] Kim D C, Lee M J, Ahn S E, Seo S, Park J C, Yoo I K, Baek I G, *et al.* 2006 *Appl. Phys. Lett.* **88** 232106

[21] Sharma S, Tomar M, Kumar A, Puri N K and Gupta V 2015 *J. Appl. Phys.* **118** 074103

[22] Zhang J X, Zheng H W, Zhang Y G, Yuan G L, Gao W X, Liu X Y, Yin G S, Gu Y Z and Zhang W F 2015 *Mater. Lett.* **156** 98

[23] Jiang W, Cai W, Lin Z and Fu C 2013 *Mater. Res. Bull.* **48** 3092

[24] Zhang F, Li M Y, Zhu Y, Zhao M, Xie S, Wei M, Li Y, Hu Z and Li M 2017 *J. Alloys Compd.* **695** 3178

[25] Roy S and Majumder S B 2012 *J. Alloys Compd.* **538** 153

[26] Zhang L, Chen J, Fan L and Pan Z 2018 *J. Alloys Compd.* **742** 351

[27] Kinoshita K, Tamura T, Aoki M, SugiyamaY and Tanaka H 2006 *Appl. Phys. Lett.* **89** 103509

[28] Biju K P, Liu X, Siddik M, Kim S, Shin J, Kim I, Ignatiev A and Hwang H 2011 *J. Appl. Phys.* **110** 064505

[29] Peng H Y, Li G P, Ye J Y, Wei Z P, Zhang Z, Wang D D, Xing G Z and Wu T 2010 *Appl. Phys. Lett.* **96** 192113

[30] Hao L, Xue Q, Gao X, Li Q, Zheng Q and Yan K 2007 *Appl. Phys. Lett.* **91** 212105

[31] Liu G, Jaegermann W, He J, Sundström V and Sun L 2002 *J. Phys. Chem. B* **106** 5814

[32] Paudel T R, Jaswal S S and Tsymbal E Y 2012 *Phys. Rev. B* **85** 104409

[33] Tsurumaki A, Yamada H and Sawa A 2012 *Adv. Funct. Mater.* **22** 1040